

Cite this: *Phys. Chem. Chem. Phys.*, 2012, **14**, 529–537

www.rsc.org/pccp

PAPER

Chemical dynamics of the $\text{CH}(\text{X}^2\Pi) + \text{C}_2\text{H}_4(\text{X}^1\text{A}_{1g})$, $\text{CH}(\text{X}^2\Pi) + \text{C}_2\text{D}_4(\text{X}^1\text{A}_{1g})$, and $\text{CD}(\text{X}^2\Pi) + \text{C}_2\text{H}_4(\text{X}^1\text{A}_{1g})$ reactions studied under single collision conditions

Fangtong Zhang, Pavlo Maksyutenko and Ralf I. Kaiser*

Received 19th July 2011, Accepted 11th October 2011

DOI: 10.1039/c1cp22350j

The crossed beam reactions of the methylidyne radical with ethylene ($\text{CH}(\text{X}^2\Pi) + \text{C}_2\text{H}_4(\text{X}^1\text{A}_{1g})$), methylidyne with D4-ethylene ($\text{CH}(\text{X}^2\Pi) + \text{C}_2\text{D}_4(\text{X}^1\text{A}_{1g})$), and D1-methylidyne with ethylene ($\text{CD}(\text{X}^2\Pi) + \text{C}_2\text{H}_4(\text{X}^1\text{A}_{1g})$) were conducted at nominal collision energies of 17–18 kJ mol^{-1} to untangle the chemical dynamics involved in the formation of distinct C_3H_4 isomers methylacetylene (CH_3CCH), allene (H_2CCCH_2), and cyclopropene ($\text{c-C}_3\text{H}_4$) via C_3H_5 intermediates. By tracing the atomic hydrogen and deuterium loss pathways, our experimental data suggest indirect scattering dynamics and an initial addition of the (D1)-methylidyne radical to the carbon–carbon double bond of the (D4)-ethylene reactant forming a cyclopropyl radical intermediate ($\text{c-C}_3\text{H}_5/\text{c-C}_3\text{D}_4\text{H}/\text{c-C}_3\text{H}_4\text{D}$). The latter was found to ring-open to the allyl radical ($\text{H}_2\text{CCHCH}_2/\text{D}_2\text{CCHCD}_2/\text{H}_2\text{CCDCH}_2$). This intermediate was found to be long lived with life times of at least five times its rotational period and decomposed via atomic hydrogen/deuterium loss from the central carbon atom (C2) to form allene via a rather loose exit transition state in an overall strongly exoergic reaction. Based on the experiments with partially deuterated reactants, no compelling evidence could be provided to support the formation of the cyclopropene and methylacetylene isomers under single collision conditions. Likewise, hydrogen/deuterium shifts in the allyl radical intermediates or an initial insertion of the (D1)-methylidyne radical into the carbon–hydrogen/deuterium bond of the (D4)-ethylene reactant were found to be—if at all—of minor importance. Our experiments propose that in hydrocarbon-rich atmospheres of planets and their moons such as Saturn's satellite Titan, the reaction of methylidyne radicals should lead predominantly to the hitherto elusive allene molecule in these reducing environments.

1. Introduction

It is well documented that resonantly stabilized free radicals (RSFRs) such as the propargyl (H_2CCCH) and allyl radical (H_2CCHCH_2) play a crucial role in the formation of aromatic molecules in combustion flames and possibly in hydrocarbon-rich atmospheres of planets and their moons.^{1–4} These radicals possess multiple resonance structures that correspond to the same arrangement of the nuclei of the atoms.⁵ Thus RSFRs are thermodynamically more stable than non-resonant radicals like methyl (CH_3) and ethyl (C_2H_5).⁵ This stability has three important implications: (1) stable hydrocarbons preferentially decompose to resonantly stabilized radicals rather than to non-resonant radicals, (2) resonantly stabilized radicals react with molecular oxygen (O_2) more slowly than non-resonant radicals, and (3) resonantly stabilized radicals dissociate less preferentially than non-resonant radicals.¹ Consequently, resonantly

stable radicals formed rapidly, but have low destruction rates in hydrocarbon flames and often accumulate to high concentrations. Not surprisingly, the formation and stability (unimolecular decomposition) of the allyl radical (C_3H_5 , X^2A_1) as one of the two prototype examples of resonantly stabilized radicals—the other being the propargyl radical (C_3H_3 , X^2B_2)—received significant interest during the last few decades. Fischer and Chen⁶ and Morton *et al.*⁷ detected the atomic hydrogen and deuterium atom loss associated with allene production at 193 nm. Follow-up photodissociation studies at 248 nm and 351 nm under collision-less conditions by Stranges *et al.* in 1998⁸ and 2008⁹ verified the presence of the atomic hydrogen loss as the main channel (84% and 95%, respectively), but also implied the importance of the methyl plus acetylene ($\text{CH}_3 + \text{C}_2\text{H}_2$) channel. Statistical RRKM calculations on the allyl radical photodissociation at 248 nm presented similar branching ratios predicting 98% of the atomic hydrogen loss channel (mainly allene) and 2% of methyl plus acetylene. Theoretically, the C_3H_5 potential energy surface was also investigated by Davis *et al.*,¹⁰ Sirjean *et al.*,¹¹ Miller *et al.*,¹² and Hostettler *et al.*¹³ probing

Department of Chemistry, University of Hawai'i at Mānoa, Honolulu, Hawaii 96822, USA. E-mail: ralfk@hawaii.edu

atomic hydrogen loss pathways to allene/methylacetylene, the methyl plus acetylene channel, and isomerization of cyclopropyl to allyl. Miller *et al.*¹² also calculated rate coefficients for the reactions of atomic hydrogen with allene and methylacetylene and tackled the isomerization of cyclopropyl to allyl followed by a thermal dissociation of the propenyl and allyl radicals.

Experimentally, the C_3H_5 potential energy surface (PES) is accessible through the reaction of the methylidyne radical (CH , $X^2\Pi$) with the ethylene molecule (C_2H_4 , X^1A_{1g}). Due to the barrier-less nature of this reaction associated with rapid rate constants in the order of $10^{-10} \text{ cm}^3 \text{ s}^{-1}$ down to 10 K, this bimolecular reaction was suggested to play an important role in planetary and interstellar chemistry.^{3,14} These kinetics studies suggest that as a photodissociation product of methane,¹⁴ the reaction of methylidyne with ethylene proceeds either *via* methylidyne insertion to form an allyl radical or by methylidyne addition to the olefinic carbon-carbon double bond yielding a cyclopropyl radical.^{15,16} However, the true nature of the nascent reaction products under single collision conditions has remained elusive. In detail, Berman *et al.*¹⁷ first measured the rate constant of this system monitoring the decay of the laser-induced fluorescence signal at 430 nm. The rate constants for the reactions of ethynyl with ethylene were found to increase with decreasing temperature. These rate constants were measured between 160 and 652 K and could be fit with the relationship $k = (2.23 \pm 0.27) \times 10^{-10} \exp[(173 \pm 35)/T] \text{ cm}^3 \text{ molecule}^{-1} \text{ s}^{-1}$. In 1984, the first *ab initio* study of this system was performed by Gosavi *et al.*¹⁶ at the CISDQ/6-31G//ROHF/6-31G level. The addition reaction was predicted to occur without an energy barrier, which was assumed to be consistent with the small negative temperature coefficient observed by Berman *et al.* For the insertion, an energy barrier as high as 63 kJ mol^{-1} was predicted, which implied that the insertion was not as important as the addition. Wang and Huang¹⁵ re-investigated the insertion pathway. This study found that the energy barrier became lower utilizing CAS calculations and disappeared with MP2 calculations. Their results indicate that insertion is also energetically feasible. In 1997 this reaction was studied at low temperature between 23 and 295 K utilizing a CRESU apparatus by Canosa *et al.*¹⁸ They found that this reaction remained very fast at low temperature, a maximum rate was obtained at about 70 K and then the rate coefficients slightly decreased at lower temperature. In 2001, Thiesemann *et al.*¹⁹ probed the temperature dependence and deuterium kinetic isotope effects in the CH (CD) + C_2H_4 (C_2D_4) reactions between 295 and 726 K. The overall rate coefficients for these reactions were determined in the pressure range of 15 Torr to 200 Torr and a temperature range of 290 K to 720 K. The slight negative temperature dependences of the rate coefficients are typical for barrier-less association reactions with subsequent fast decay of the collision complex. The kinetic isotope effect of the deuteration of the ethylene reagent of $8 \pm 3\%$ did not allow a clear experimental differentiation between the competing addition and insertion pathways, but quantum chemical calculations suggest that insertion is a minor channel, *i.e.* 10% at most at a temperature of 800 K. In 2003, McKee *et al.*²⁰ studied the hydrogen atom branching ratios of the methylidyne-ethylene system at room temperature and 25 Torr. The hydrogen atoms

were detected *via* Lyman α laser induced resonance fluorescence at 121.56 nm. The branching ratio they observed was 1.09 ± 0.14 suggesting that under these experimental conditions, the atomic hydrogen loss is the only reaction pathway. This examination also discussed the likely reaction mechanism and concluded that the fate of any cyclopropyl radical was likely to be conversion into the thermodynamically more stable allyl radical. An elimination of the hydrogen atom from the central carbon atom would lead then to the formation of allene. They also predicted cyclopropene to be produced in negligible amounts. This study also suggested that a 2,1-H shift in the allyl radical formed the 2-propenyl radical (CH_3CCH_2), which can then decompose to either methylacetylene or allene, with a lower energy barrier toward methylacetylene formation. The instantaneous hydrogen atom elimination from the allyl radical is expected to be 10 times faster than the 2,1-H shift. In 2009 Loison and Bergeat²¹ re-investigated the rate constant and the hydrogen atom branching ratio of this reaction. The overall rate constant at 300 K was found to be $(3.1 \pm 0.6) \times 10^{-10} \text{ cm}^3 \text{ molecule}^{-1} \text{ s}^{-1}$ with the atomic hydrogen branching ratio being 0.94 ± 0.08 . In the same year, Goulay *et al.*²² studied the formation of cyclic (cyclopropene) *versus* acyclic (allene, methylacetylene) isomers produced at room temperature utilizing photoionization of the products formed; their study indicated that the C_3H_5 intermediate decayed *via* atomic hydrogen loss to yield $70 \pm 8\%$ allene, $30 \pm 8\%$ methylacetylene, and less than $10 \pm 10\%$ cyclopropene. However, in all previous kinetics studies, the nature of the nascent reaction products formed *under single collision conditions* has never been investigated so far. More recently, Chen *et al.*^{23,24} re-investigated the photodissociation dynamics of the allyl radical by focusing on the methyl (CH_3) loss channel. By trajectory calculations and a refitting of Strange *et al.*'s experimental data⁹ of 248 nm photodissociation of the partially deuterated 2-D1-allyl radical, they identified the production of vinylidene (CCH_2) as well as two distinctly different mechanisms to form methyl and acetylene products. Their results also predicted the primary dissociation channel to be hydrogen loss with a quantum yield of 0.94 forming either allene or propyne with a ratio of 6.4 : 1. Methyl and acetylene are produced with a quantum yield of 0.06 by three different mechanisms (the vinylidene eventually isomerizes to give internally excited acetylene).

Here, we report for the first time on the unimolecular decomposition of chemically activated C_3H_5 intermediates together with its partially deuterated counterparts, which are formed under single collision conditions in the crossed beam reactions of methylidyne with ethylene ($CH(X^2\Pi) + C_2H_4(X^1A_{1g})$), methylidyne with D4-ethylene ($CH(X^2\Pi) + C_2D_4(X^1A_{1g})$), and D1-methylidyne with ethylene ($CD(X^2\Pi) + C_2H_4(X^1A_{1g})$). This study also sheds light on the underlying chemical dynamics of this reaction forming distinct C_3H_4 isomers in combustion flames in hydrocarbon rich atmospheres of planets and their moons.

2. Experimental and data analysis

The elementary reactions of the (D1)-methylidyne radical, (CD/CH ; $X^2\Pi$), with ethylene (C_2H_4 ; X^1A_1) and D4-ethylene (C_2D_4 ; X^1A_1) were performed in a universal crossed molecular

beams machine under single collision conditions.^{25–29} Briefly, a supersonic beam of methylidyne/D1-methylidyne radicals was generated in the primary source chamber *via* photodissociation of (D1)-bromoform (CDBr₃/CHBr₃; 99.5%, Aldrich), which was seeded in helium (99.9999%, Airgas) at fractions of about 0.1%. This gas mixture was formed by passing 2.2 atm helium gas through liquid (D1)-bromoform stored in a stainless steel bubbler, which was kept in a 283 K cooling bath. The gas mixture was then released by a Proch-Trickl pulsed valve operating with a 0.96 mm nozzle at 60 Hz, 80 μs pulse width, and –400 to –450 V pulse amplitude. The distance between the pulsed valve and skimmer was optimized to 13 ± 1 mm. (D1)-bromoform molecules were then photodissociated by a 248 nm laser beam from a Lambda Physik Compex 110 Excimer laser operated at 30 Hz. The laser beam had an energy of 60 mJ per pulse and was focused by a quartz lens with 1 m focal length to 4 mm by 0.7 mm before intercepting the molecular beam perpendicularly about 5 mm downstream of the nozzle. Under our operation conditions, CD/CH(X²Π) radicals were only in their ground state once reaching the crossing region of the main chamber, since the lifetimes of the A and B states of methylidyne are 440 ± 20 ns and 470 ± 20 ns respectively; any excited state species would relax before reaching the skimmer. A four-slot chopper wheel installed after the skimmer selected a part of the (D1)-methylidyne beam at a defined peak velocity (v_p) of about 1740 ms⁻¹ (Table 1). A few 10¹² radicals cm⁻³ per pulse were present in the interaction region crossing a pulsed ethylene/D4-ethylene beam (C₂D₄, 99% D enrichment, CDN; 550 Torr) released by a second pulsed valve perpendicularly. In order to optimize the intensity of each supersonic beam, which strongly depends on the distance between the pulsed valve and the skimmer, on line and *in situ*, each pulsed valve was placed on an ultra high vacuum compatible micro positioning translation stages with three stepper motors (New Focus). This allows monitoring the beam intensity *versus* the position of the pulsed valve in each source chamber in real time.

The characteristics of the methylidyne beam was also studied *via* laser induced fluorescence (LIF) monitoring the A²Δ–X²Π transition,^{25,30} the results suggest a rotational temperature of 14 ± 1 K in the vibrational ground state; less than 6% of the radicals are in the first vibrationally excited state population. It should be addressed that the photodissociation of bromoform at 248 nm is a complicated multi-photon process. Along with methylidyne radicals, other species like CHBr₂, CHBr, CBr, and atomic carbon and bromine could exist in the beam. However, due to the much heavier bromine atom, these bromine containing species would generate products with distinctively

different mass to charge ratios and center of mass angle much closer to the primary beam; therefore, these species would not interfere with the methylidyne reactions. The carbon atom is lighter than the methylidyne radical, thus it does not affect the data taken at $m/z = 40$ (C₃H₄⁺), since reactive scattering of carbon atoms with ethylene can only yield a product at $m/z = 39$ (C₃H₃⁺).^{25,30}

The reactively scattered products were monitored using a triply differentially pumped quadrupole mass spectrometric detector in the time-of-flight (TOF) mode after electron-impact ionization of neutral species at 80 eV electron energy. This detector can be rotated within the plane defined by the primary and the secondary reactant beams to allow taking angular resolved TOF spectra. At each angle, up to 1 × 10⁶ TOF spectra (up to 10 hours per angle) were accumulated. The recorded TOF spectra were then integrated and normalized to extract the product angular distribution in the laboratory frame (LAB). In this setup, both the primary and secondary pulsed valves were operated at 60 Hz, but the photodissociation laser at only half the repetition rate of 30 Hz. This allows a background subtraction by taking TOF spectra in the ‘laser on’ mode and subtracting from the TOF spectra recorded on the ‘laser off’ mode. To extract information on the reaction dynamics, the experimental data must be transformed into the center-of-mass reference frame utilizing a forward-convolution routine.^{31,32} This iterative method initially assumes an angular flux distribution, $T(\theta)$, and the translational energy flux distribution, $P(E_T)$, in the center-of-mass system (CM). Laboratory TOF spectra and the laboratory angular distributions (LAB) were then calculated from the $T(\theta)$ and $P(E_T)$ function and were averaged over a grid of Newton diagrams to account for the apparatus functions and the beam spreads. Each diagram defines, for instance, the velocity and angular spread of each beam and the detector acceptance angle. Best fits were obtained by iteratively refining the adjustable parameters in the center-of-mass functions within the experimental error limits of, for instance, peak velocity, speed ratio, error bars in the LAB distribution.

3. Results

3.1. Laboratory data

For the CH + C₂H₄ system, the signal was monitored for $m/z = 40$ and 39 corresponding to ions with the molecular formula C₃H₄⁺ ($m/z = 40$) and C₃H₃⁺ ($m/z = 39$). Since the primary beam also contained ground state carbon atoms, which reacted with ethylene *via* atomic hydrogen loss to form the propargyl radical (C₃H₃),³³ this channel also contributed to the reactive scattering signal recorded at $m/z = 39$. Therefore, the time-of-flight spectra and laboratory angle distributions recorded at a mass-to-charge ratio of $m/z = 39$ were slightly different from those recorded at $m/z = 40$; up to about 10% of the signal at $m/z = 39$ signals contributed from reactive scattering of ground state carbon atoms with ethylene as studied earlier.³³ The raw data recorded at $m/z = 40$ suggest that a molecule of the chemical formula C₃H₄ represented the reaction product formed *via* an atomic hydrogen loss pathway. Secondly, ions at $m/z = 39$ were formed *via*

Table 1 Primary and secondary beam peak velocities (v_p), speed ratios (S), collision energies (E_c), and center-of-mass angles (θ_{CM})

Beam	v_p/ms^{-1}	S	$E_c/\text{kJ mol}^{-1}$	θ_{CM}
CH(X ² Π)	1738 ± 12	16.0 ± 0.5	—	—
C ₂ H ₄ (X ¹ A _{1g})	905 ± 20	10.0 ± 0.2	17.1 ± 0.3	48.3 ± 0.5
CH(X ² Π)	1738 ± 12	16.0 ± 0.5	—	—
C ₂ D ₄ (X ¹ A _{1g})	880 ± 20	10.0 ± 0.2	17.5 ± 0.3	51.3 ± 0.5
CD(X ² Π)	1738 ± 11	14.7 ± 0.5	—	—
C ₂ H ₄ (X ¹ A _{1g})	900 ± 20	10.0 ± 0.2	17.8 ± 0.3	46.0 ± 0.5

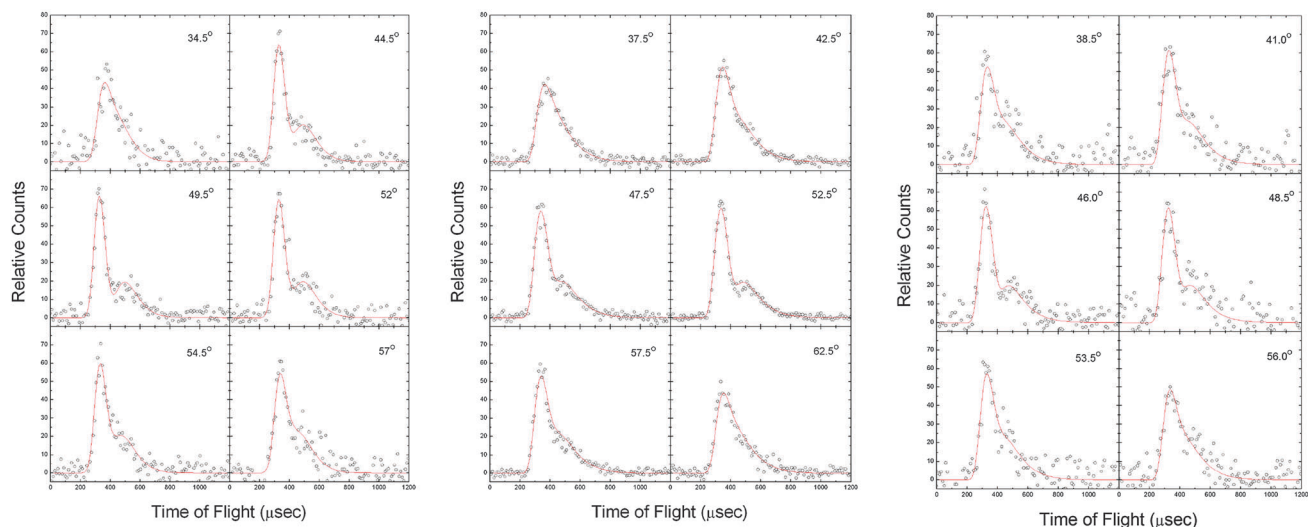


Fig. 1 Selected time-of-flight (TOF) spectra taken at mass-to-charges, m/z , of 40 (C_3H_4^+) (left), 42 (C_3D_3^+) (center), and 40 (C_3H_4^+) (right) in the reactions of methylidyne with ethylene, methylidyne with D4-ethylene, and D1-methylidyne with ethylene. Circles indicate the experimental data, the solid lines the calculated fits.

dissociative ionization of the parent C_3H_4 molecule in the electron impact ionizer (about 90%) plus the contribution from ionized C_3H_3 synthesized in the reaction of carbon with ethylene (about 10%). Finally, no molecular hydrogen loss channel could be monitored at $m/z = 39$ under our experimental conditions. Consequently, for the $\text{CH} + \text{C}_2\text{H}_4$ system, only the atomic hydrogen loss pathway is open within this mass range. The corresponding TOF and LAB angular distributions of C_3H_4^+ ($m/z = 40$) are depicted in Fig. 1 and 2, respectively. It should be noted that at angles closer to the primary beam, we observed at $m/z = 40$ and 39 interference from non-reactively scattered, doubly charged $^{81}\text{Br}^{2+}$ ($m/z = 40.5$)

and $^{79}\text{Br}^{2+}$ ($m/z = 39.5$). Our mass spectrometer was operated at a resolution of 1 amu to discriminate, for instance, the signal at $m/z = 40$ from $m/z = 39$. These settings allowed that non-reactively scattered, doubly ionized $^{81}\text{Br}^{2+}$ ($m/z = 40.5$) and ^{79}Br ($m/z = 39.5$) leaked into $m/z = 40$. An operation of the mass spectrometer at a resolution of 0.5 amu, which would have avoided this complication, was impractical as the reactive scattering signal at $m/z = 40$ and 39 at a resolution of 0.5 amu was found to diminish beyond an acceptable intensity. However, the effect of the non-reactively scattered species on the laboratory data could be investigated by measuring the signal at $m/z = 40$ and 39 utilizing neon carrier gas as the secondary

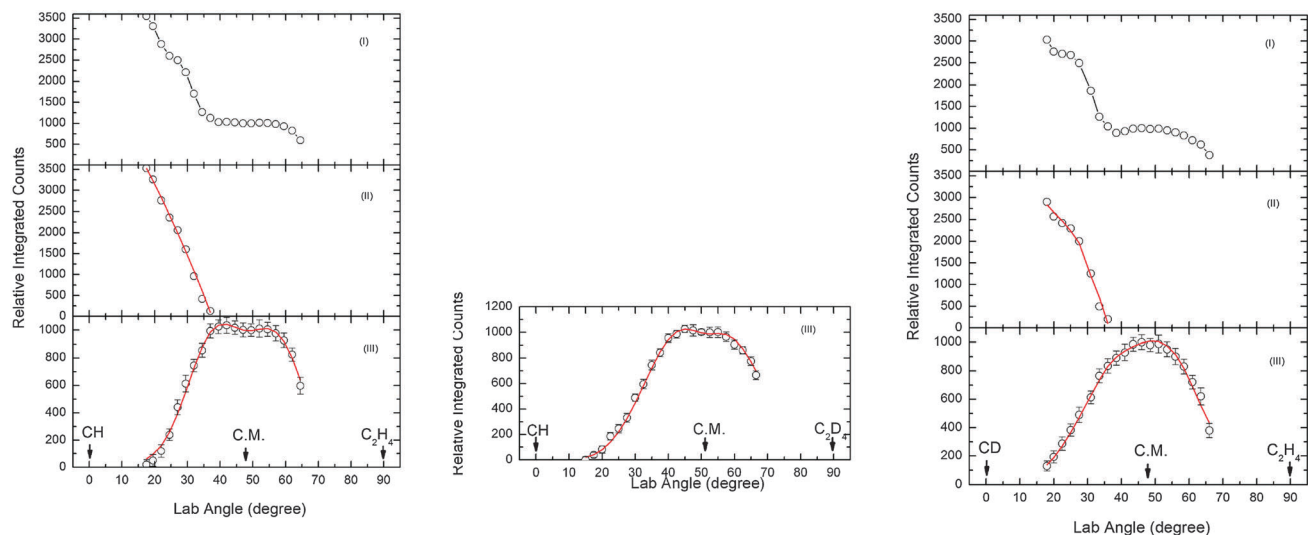


Fig. 2 Laboratory angular distributions taken at mass-to-charge ratios, m/z , of 40 (C_3H_4^+) (left), 42 (C_3D_3^+) (center), and 40 (C_3H_4^+) (right) in the reactions of methylidyne with ethylene, methylidyne with D4-ethylene, and D1-methylidyne with ethylene. Circles indicate the experimental data, the solid lines the calculated fits. CM designates the center-of-mass angle. For the methylidyne/ethylene (left) and D1-methylidyne/ethylene (right) systems, the upper panel shows the total ion counts for the signal at $m/z = 40$, the center panel ion counts for the signal at $m/z = 40$ from non-reactively scattered doubly ionized bromine, and the bottom panels the difference (see text for a detailed discussion).

beam to obtain the non-reactive scattering signal. Thus, the subtraction of this signal revealed the laboratory angular distributions and time-of-flight data of the reactive scattering signal for the reaction of methylidyne with ethylene. Here, the laboratory angular distribution of $m/z = 40$ is quite wide and spreads over at least 60° within the scattering plane. Further, the laboratory angular distribution peaks close to the center-of-mass angle of the system and shows a slight dip at the latter. These results suggest that the reaction likely proceeds *via* indirect scattering dynamics *via* complex formation.

For the $\text{CH} + \text{C}_2\text{D}_4$ reaction, due to the high background at $m/z = 44$ (from CO_2^+ formed *via* ion–molecule reactions of CO with CO^+ ion in the ionizer of the detector), the reactive scattering signal could not be monitored for C_3D_4^+ ($m/z = 44$). No background interference was observed at $m/z = 43$ ($\text{C}_3\text{D}_3\text{H}^+$), *i.e.* a potential deuterium atom loss; nevertheless, no signal was observed at this mass-to-charge ratio. However, we were able to observe the signal at $m/z = 42$ (C_3D_3^+). The TOF spectra and laboratory angular distributions taken at $m/z = 42$ are shown in Fig. 1 and 2, respectively; note that no interference from doubly charged $^{81}\text{Br}^{2+}$ ($m/z = 40.5$) and $^{79}\text{Br}^{2+}$ ($m/z = 39.5$) was present. The raw data (TOF, LAB) depict similar pattern to those of the $\text{CH} + \text{C}_2\text{H}_4$ reaction. Best fits of data at $m/z = 42$ (C_3D_3^+) could be only achieved with a mass combination of 44 amu (C_3D_4) plus 1 amu (H), but not for the combination of 42 amu (C_3D_3) plus 3 amu (HD) (Section 3.2). Therefore, we suggest for the $\text{CH} + \text{C}_2\text{D}_4$ reaction, within the limits of our fits, the presence of the atomic hydrogen loss leading to C_3D_4 , but the absence of the molecular hydrogen loss (here in form of HD) pathway within our signal to noise.

Finally, for the $\text{CD} + \text{C}_2\text{H}_4$ reaction, the reactive scattering signal was observed at $m/z = 40$ (C_3H_4^+), but not at $m/z = 41$ ($\text{C}_3\text{H}_3\text{D}^+$). Background interferences from non-reactively scattered bromine in the form of $^{81}\text{Br}^{2+}$ ($m/z = 40.5$) were accounted for as described above. Best fits of data at $m/z = 40$ (C_3H_4^+) were obtained with a mass combination of 40 amu (C_3H_4)

plus 2 amu (D). Consequently, we can conclude that the reaction of D1-methylidyne with ethylene leads to C_3H_4 isomers plus atomic deuterium. Similar to the $\text{CH} + \text{C}_2\text{H}_4$ and $\text{CH} + \text{C}_2\text{D}_4$ reaction, no molecular ‘hydrogen’ channel was observed.

3.2. Center of mass angular, $T(\theta)$, and translational energy, $P(E_T)$, distributions

For the $\text{CH} + \text{C}_2\text{H}_4$ system, the recorded TOF spectra and laboratory angular distribution at $m/z = 40$ (C_3H_4^+) could be fit with a single channel of the product mass combination 40 amu (C_3H_4) plus 1 (H) amu by utilizing a parameterized center-of-mass angular distribution and a center-of-mass translational energy distribution in point form. The derived center-of-mass functions are shown in Fig. 3. The center of mass angular distribution, $T(\theta)$, depicts intensity over the complete angular range from 0° to 180° ; further, the best fit is slightly forward scattered and holds a small maximum at 90° . These findings indicate that the $\text{CH} + \text{C}_2\text{H}_4$ reaction involves indirect scattering dynamics *via* the formation of a bound C_3H_5 reaction intermediate(s).³⁴ Also, the very slightly forward shaped $T(\theta)$ with typical intensities of $I(180^\circ)/I(0^\circ) \approx 0.9 \pm 0.1$ suggests that the life time of the intermediate(s) is longer than the rotational period; within the limits of the oscillating complex model, life times of about five times the rotational period of the C_3H_5 can be proposed.³⁵ Since the rotational period of this C_3H_5 intermediate is estimated as 0.2, 0.9 and 1.0 ps for A , B , C axes, respectively, the life time of this complex is estimated to be 1, 4.5 and 5 ps, where t_{rot} is the rotational period, I_i is the moment of inertia of the complex rotating around the i axis ($i = A, B, C$), μ is the reduced mass of the reactants, b_{max} is the maximum impact parameter, v_{rel} is the relative velocity of the reactants and τ is the rotational period.³⁵

$$t_{\text{rot}} = 2\pi I_i / L_{\text{max}} = 2\pi I_i / (\mu \times b_{\text{max}} \times v_{\text{rel}}) \quad \langle i = A, B, C \rangle \quad (1)$$

$$\tau = -t_{\text{rot}} / (2 \ln(I(180^\circ)/I(0^\circ))) \quad (2)$$

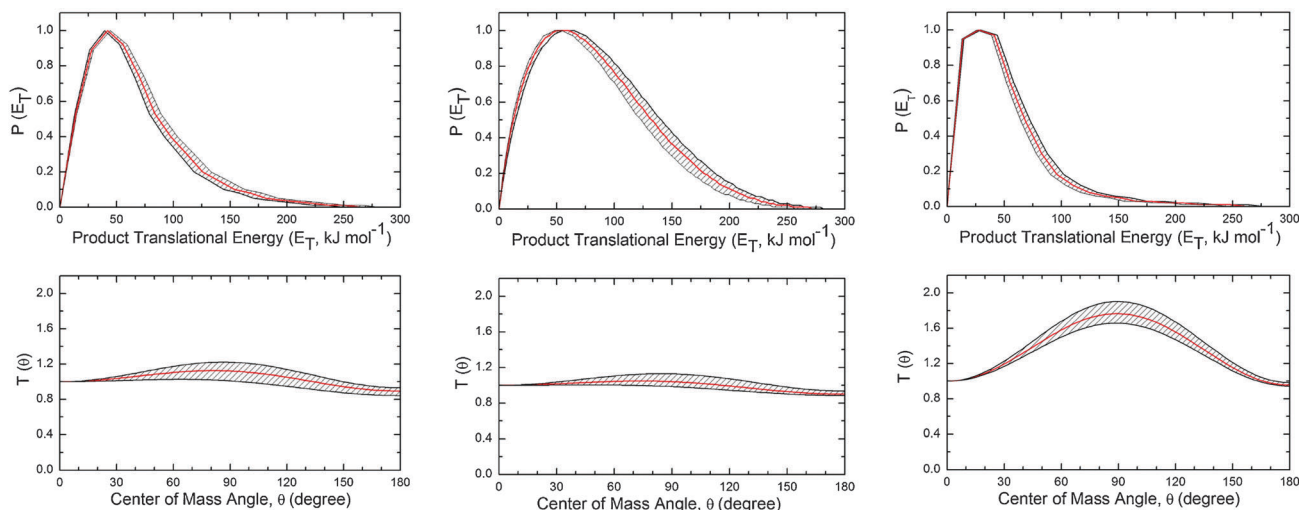


Fig. 3 Center-of-mass angular (bottom) and translational energy flux distributions (top) derived for the product combinations $\text{C}_3\text{H}_4 + \text{H}$, $\text{C}_3\text{D}_4 + \text{H}$, and $\text{C}_3\text{H}_4 + \text{D}$ for the reactions of methylidyne with ethylene, methylidyne with D4-ethylene, and D1-methylidyne with ethylene, respectively. Best fit functions are shown in red, whereas the hatched areas depict the error limits.

The center-of-mass translational energy distribution, $P(E_T)$, provides us with additional information on the reaction dynamics. For this system, the $P(E_T)$ extends up to a maximum translational energy of 275 kJ mol^{-1} (Fig. 3). Adding or subtracting 20 kJ mol^{-1} does not change the fit significantly. Since the high energy cutoff presents the sum of the absolute reaction energy and the collision energy, we can subtract the collision energy to compute the reaction to be exoergic by $258 \pm 20 \text{ kJ mol}^{-1}$. Secondly, the $P(E_T)$ has a broad peak maximum at about $30\text{--}40 \text{ kJ mol}^{-1}$. This finding suggests that at least one exit channel holds a tight exit barrier upon decomposition of the C_3H_5 intermediate(s). By integrating the center-of-mass translational energy distribution and accounting for the available energy, the average fraction of available energy channeling into the translational degrees of freedom is computed to be $27 \pm 3\%$. This order of magnitude indicates indirect scattering dynamics *via* complex formation as already predicted from the center-of-mass angular distributions. For the $\text{CH} + \text{C}_2\text{D}_4$ system, the experimental results at $m/z = 42$ were fit with a single channel with the mass combination of 44 (C_3D_4) and 1 (H) amu. The center of mass angular distribution is within the error limits very similar to the function derived for the $\text{CH} + \text{C}_2\text{H}_4$ system suggesting indirect scattering dynamics and a life time of the $\text{C}_3\text{D}_4\text{H}$ intermediate, decomposing *via* atomic hydrogen loss to the C_3D_4 product, of at least five times of its rotational period. The center-of-mass translational energy distribution is quite similar to the one for the $\text{CH}/\text{C}_2\text{H}_4$ system. The $P(E_T)$ shows a pronounced distribution maximum at about 50 kJ mol^{-1} , which is indicative of a tight exit transition state. Also, the high energy cutoff proposed a reaction energy of about $259 \pm 20 \text{ kJ mol}^{-1}$ with the average fraction of available energy channeling into the translational degrees of freedom of $31 \pm 3\%$. Finally, laboratory data for the $\text{CD}/\text{C}_2\text{H}_4$ system could be also replicated with a single channel (center-of-mass angular and translational energy distributions in parameter and point form, respectively) with the mass combination of 40 (C_3H_4) and 2 (D) amu. The center of mass translational energy distribution is very close to those derived for the $\text{CH}/\text{C}_2\text{H}_4$ system indicating that the signal at $m/z = 44$ presents the reactive scattering signal to form C_3H_4 *via* atomic deuterium ejection. However, the center-of-mass angular distribution shows pronounced differences compared to the $\text{CH}/\text{C}_2\text{H}_4$ and $\text{CH}/\text{C}_2\text{D}_4$ systems depicting a pronounced distribution maximum at 90° with intensities at 90° *versus* 0° of 1.8 ± 0.2 . Note that in this system, the leaving atom (deuterium) has a mass twice of the atomic hydrogen, *i.e.* the light fragment lost in the $\text{CH}/\text{C}_2\text{H}_4$ and $\text{CH}/\text{C}_2\text{D}_4$ reaction. Since the final orbital angular momentum L' is the product of the 'exit' impact parameter, the relative velocity of the departing products, and the reduced mass of the products, we expect that due to the heavier mass of the deuterium atom, the final orbital angular momentum in the D1-methylidyne-ethylene system is larger than in both other systems. Therefore, the initial (L) and final (L') orbital angular momentums are likely stronger coupled in the D1-methylidyne-ethylene system compared to the methylidyne-ethylene and methylidyne-D4-ethylene systems. This results in a more pronounced peaking and hence polarization of the center-of-mass angular distribution in the D1-methylidyne-ethylene system. Note that an enhanced coupling between the initial and final

orbital angular momentum was also documented in the boron-D6-benzene (D loss) compared to the boron-benzene (H loss) reactions.³⁶

4. Discussion

Based on a comparison of the experimentally determined reaction energies to form the C_3H_4 molecule plus atomic hydrogen ($-258 \pm 20 \text{ kJ mol}^{-1}$) with the theoretically predicted energies of -252 kJ mol^{-1} , -248 kJ mol^{-1} , and -134 kJ mol^{-1} for methylacetylene, allene, and cyclopropene, respectively, we can see that at least the allene and/or the methylacetylene isomer is formed. Based on the schematic reaction sequence (Fig. 4a), the methylidyne radical can either add to the carbon-carbon double bond or insert into the carbon-hydrogen forming the cyclopropyl (1) and/or allyl (2) radicals, respectively. A hydrogen emission from (1) and (2) leads to the cyclopropene (p1) and allene isomers (p2), respectively. Intermediate (2) can also isomerize *via* a 1,3- or 2,1-hydrogen shift to (4) and (3), respectively. As outlined in Fig. 4a, these intermediates can emit a hydrogen atom leading to allene (p2) and/or methylacetylene (p3).

Considering the data from the $\text{CH}/\text{C}_2\text{H}_4$ experiment alone, we cannot make any conclusion as to what extent p2 and p3 are formed, and if p1 might be also a minor reaction product. However, the results from the $\text{CH}/\text{C}_2\text{D}_4$ and $\text{CD}/\text{C}_2\text{H}_4$ systems help to untangle these questions. Recall that in the reaction of CH with C_2D_4 , only an atomic hydrogen loss was observed. Based on the schematic reaction sequence as compiled in Fig. 4b, the cyclopropene isomer (p1*) can only be formed *via* a deuterium atom elimination in this system from (1*). This was clearly not observed experimentally. Therefore, we can conclude that the cyclopropene molecule (p1*) is not formed in the reaction of methylidyne with D4-ethylene. Further, we attempt to answer the question if based on our data the addition or insertion pathway dominates. An insertion would lead to a D4-allyl radical (2**), which can undergo various hydrogen/deuterium shifts and also a deuterium elimination from the central carbon atom forming allene p2**. However, recall that a deuterium loss was not observed experimentally, and we can discount for the formation of p2** immediately. Similarly, the synthesis of p3* from (4**), p3*** from (4***), p2** from (3**), and p3* from (3**) can be eliminated since the deuterium loss was not observed experimentally. Therefore, the existence of intermediates (4**) and (4***), which are required if a deuterium loss is observable and which can be formed only *via* hydrogen/deuterium shifts from (2**), can be also excluded. Consequently, 1,3- and 3,1-hydrogen/deuterium shifts in (2**) likely play no role in the reaction dynamics. This conclusion can be transferred to (2*), which should not undergo a 1,3-deuterium shift either. The possible existence of (3**) deserves special attention. This intermediate should undergo—besides deuterium loss from C3—either a hydrogen or deuterium elimination from C1. Even if isotope effects play a role, an exclusive elimination of a hydrogen atom and a lack of deuterium emission from the C1 atom of (3**) are unlikely. Therefore, if (3**) is present, we would expect the observation of the deuterium loss pathway. A lack of this observation suggests that (3**) is unlikely to contribute to the hydrogen atom loss pathway. The same argument holds for (3) which can be accessed *via* (2*) or

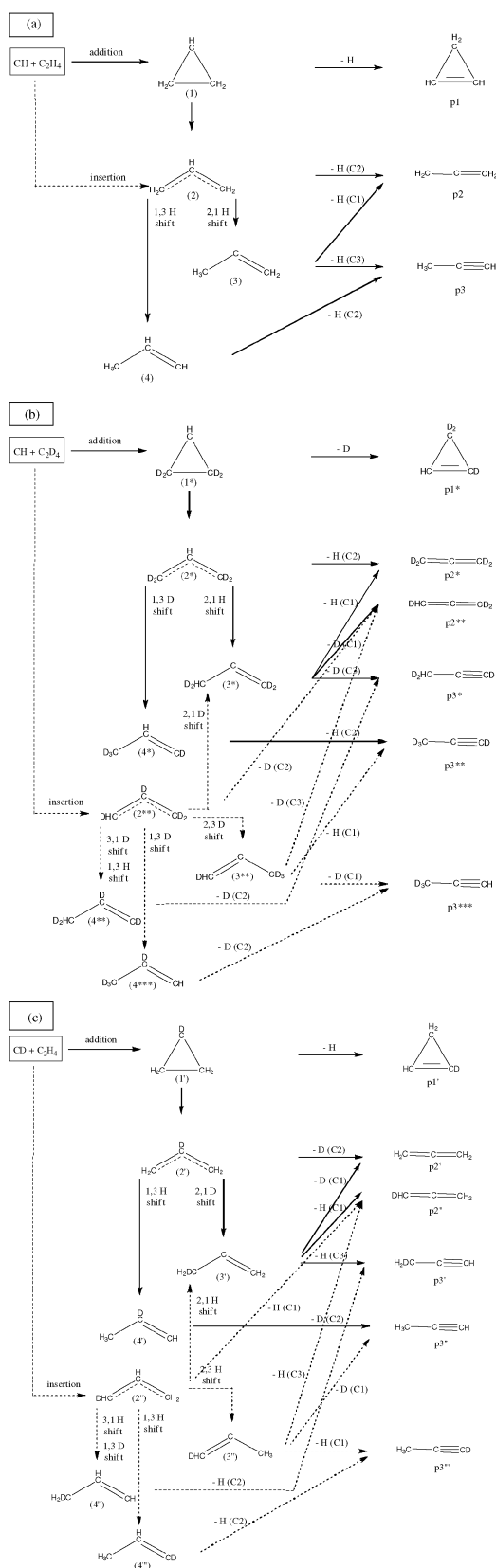


Fig. 4 Schematic representation of isotopologues and isotopomers of reaction intermediates and products accessible in the reaction of methylidyne with ethylene (a), methylidyne with D₄-ethylene (b) and D₁-methylidyne with ethylene (c). Pathways from insertion and addition processes are defined by dashed and solid lines, respectively.

from (2**) formed *via* insertion from the reactants. A unimolecular decomposition of (3*) under single collision conditions should be reflected in a hydrogen *and* deuterium ejection from C1; since no deuterium loss was observed, we can likely discount for the existence of (3*). This also suggests the absence of any CH insertion forming (2**) since all isomerization pathways from (2**) were found to play no role in the scattering dynamics. Also, a deuterium elimination from C3 can be ruled out since no deuterium loss was observed experimentally. Based on these considerations, the only remaining pathway is the atomic hydrogen loss from (2*) forming allene (p2*) under single collision conditions. To summarize, the results in the CH/C₂D₄ system suggest that the methylidyne radical adds to the carbon-carbon double bond of the D₄-ethylene reactant leading to a cyclopropyl radical (1*), which ring opens to allyl (2*). The latter emits a hydrogen atom from the C2 position forming allene (p2*). The formation of cyclopropene (p1*) can be discounted for due to the lack of any deuterium emission. The insertion process is—if it plays a role—only of minor importance, according to the experimental observations—most important the lack of deuterium atom emission from distinct reaction intermediates. The same arguments hold for the formation of any methylacetylene products (p3*/p3**): here, all pathways leading to methylacetylene (p3*) should result in the observation of atomic deuterium as well; the route forming methylacetylene (p3**) was discounted due to the absence of intermediate (3**). Note that the results from the CD/C₂H₄ system support the conclusions (Fig. 4c). Recall that in this reaction, only an atomic deuterium elimination was observed within the signal to noise limitations of our setup. Here, the absence of a hydrogen atom loss can eliminate the formation of cyclopropene (p1') together with methylacetylene (p3'''/p3') and allene (p2''). Note that p3''' can only be formed from (3'') and (4'). The potential existence of (3'') should be also reflected in a deuterium atom loss from C1, which was not observed. On the other hand, the presence of a 1,3 hydrogen shift in (2) producing (4') can also be eliminated based on arguments for the CH/C₂D₄ system as described above.

Can these conclusions derived from the crossed beam experiments with partially deuterated reactants be supported by electronic structure calculations as compiled in Fig. 5? Our experimental finding of a predominant addition *versus* insertion process can be understood in terms of a reduced cone of acceptance of the carbon-hydrogen/deuterium σ -bond compared to the π -electrons of the carbon-carbon double bond. Further, the absence of cyclopropene formation could be rationalized since the initial addition complex cyclopropyl (1) rather ring opens *via* a barrier of 92–105 kJ mol⁻¹ compared to decomposition to cyclopropene plus atomic hydrogen, which requires more than twice the energy (211–226 kJ mol⁻¹). How about the hydrogen shifts in the allyl radical (2) formed *via* ring opening from cyclopropyl (1)? The 1,3- and 2,1-hydrogen migrations have to overcome significant isomerization barriers of about 258 and 267 kJ mol⁻¹ *via* tight transition states compared to relatively loose exit transition states located 251 kJ mol⁻¹ above the allyl radical (2), and only 2–13 kJ mol⁻¹ above the separated reactants. This makes the hydrogen elimination pathway from allyl (2) forming allene more competitive compared to isomerization steps *via* hydrogen shifts.

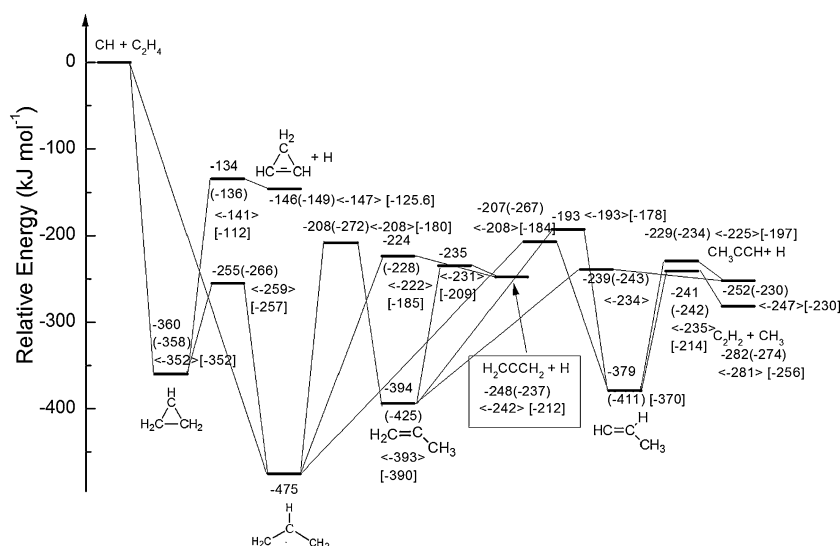


Fig. 5 Potential energy surface of the reaction of methylidyne with ethylene. Energetics are taken from ref. 12, ref. 10 (round parentheses), ref. 9 (angular brackets) and ref. 24 (square brackets). Due to the differences in zero point energies, energies for the methylidyne–D4-ethylene and D1-methylidyne–ethylene systems differ by less than 10 kJ mol⁻¹.

Finally we would like to compare our results with Chen *et al.*'s^{23,24} and Stranges *et al.*'s^{8,9} latest studies. In our system, the reaction starts with the methylidyne radical addition to the carbon–carbon double bond of ethylene to form a chemically activated, cyclic C₃H₅ intermediate found to ring-open to the allyl radical; the latter was found to predominantly emit a hydrogen atom yielding the allene molecule. Stranges *et al.*'s photodissociation study also provided conclusive evidence that the atomic hydrogen loss pathway presented the primary dissociation channel (94%); further, these studies also assigned the allene molecule as the dominating product isomer (75–80%). Further, no evidence of cyclopropene formation was reported in any study. However, there are several differences between the two studies utilizing chemically and photochemically activated C₃H₅ radicals. First, Stranges *et al.* suggested that the methyl plus acetylene pathway accounts for 6% of the total yielding; in our experiment, due to the unfavorable conditions (acetylene can be formed by dissociative ionization from the ethylene parent in the ionizer), this channel was not observable. Further, Stranges proposed that propyne accounted for 12–15% of the total yielding. Overall, our studies suggest the absence of a hydrogen migration after the formation of allyl radical, whereas this hydrogen shift was inferred in Stranges *et al.*'s^{8,9} and Chen *et al.*'s^{23,24} study due to the observation of methylacetylene. These reaction pathways need either a 1,3- or a 2,1-hydrogen migration; in the crossed beam experiments, the experimental data could be explained without these hydrogen shifts. Considering that the total available energy for the allyl radical is similar in both systems (475 + E_c = 492 kJ mol⁻¹ in our experiment and 248 nm photon is 481 kJ mol⁻¹), this difference might be due to the shorter life time of the allyl intermediate formed in the crossed beam reaction of methylidyne and ethylene (1–5 ps) compared to the photodissociation study (16 ps).²⁴ Therefore, in the crossed beam experiments the collision complex might not have a sufficient life time to permit the 1,3- or 2,1-H shift.

5. Conclusions

We conducted the crossed beam reactions of the methylidyne radical with ethylene (CH(X²Π) + C₂H₄(X¹A_{1g})), methylidyne with D4-ethylene (CH(X²Π) + C₂D₄(X¹A_{1g})), and D1-methylidyne with ethylene (CD(X²Π) + C₂H₄(X¹A_{1g})) at collision energies of 17–18 kJ mol⁻¹ to elucidate the chemical dynamics involved in the formation of distinct C₃H₄ isomers methylacetylene (CH₃CCH), allene (H₂CCCH₂), and cyclopropene (c-C₃H₄). By tracing the atomic hydrogen and deuterium loss pathways, our experimental data can be explained with indirect scattering dynamics and an initial addition of the (D1) methylidyne radical to the carbon–carbon double bond of the (D4)-ethylene reactant forming a cyclopropyl radical intermediate. The latter was found to ring-open to the allyl radical intermediate. This intermediate was found to be long lived with life times of at least five times its rotational period and decomposed *via* atomic hydrogen/deuterium loss from the central carbon atom (C2) to form the allene molecule *via* a rather loose exit transition state. Based on the deuteration pattern, we did not find any evidence for the formation of the cyclopropene molecule. Likewise, hydrogen/deuterium shifts in the allyl radical intermediates or an initial insertion of the methylidyne radical into the carbon–hydrogen/deuterium bond of the (D4)-ethylene reactant were found to be—if at all—of minor importance. Finally, our experiments suggest that in hydrocarbon-rich atmospheres of planets and their moons such as Saturn's satellite Titan, the reaction of methylidyne radicals, which are produced from photodissociation from methane,¹⁴ with ethylene should lead to the allene molecule and to a lesser extent to its methylacetylene and cyclopropene isomers.

Acknowledgements

This project was supported by the US National Science Foundation (NSF-0948258).

References

- 1 C. S. McEnally, L. D. Pfefferle, B. Atakan and K. Kohse-Hoinghaus, *Prog. Energy Combust. Sci.*, 2006, **32**, 247–294.
- 2 J. A. Miller and C. F. Melius, *Combust. Flame*, 1992, **91**, 21–39.
- 3 N. M. Marinov, W. J. Pitz, C. K. Westbrook, M. J. Castaldi and S. M. Senkan, *Combust. Sci. Technol.*, 1996, **116–117**, 211–287.
- 4 J. A. Miller, M. J. Pilling and J. Troe, *Proc. Combust. Inst.*, 2005, **30**, 43–88.
- 5 R. T. Morrison and R. N. Boyd, *Organic Chemistry*, Prentice-Hall, Englewood Cliffs, NJ, 6th edn, 1992.
- 6 I. Fischer and P. Chen, *J. Phys. Chem. A*, 2002, **106**, 4291–4300.
- 7 M. L. Morton, L. J. Butler, T. A. Stephenson and F. Qi, *J. Chem. Phys.*, 2002, **116**, 2763–2775.
- 8 D. Stranges, M. Stemmler, X. Yang, J. D. Chesko, A. G. Suits and Y. T. Lee, *J. Chem. Phys.*, 1998, **109**, 5372–5382.
- 9 D. Stranges, P. O’Keeffe, G. Scotti, R. Di Santo and P. L. Houston, *J. Chem. Phys.*, 2008, **128**, 151101.
- 10 S. G. Davis, C. K. Law and H. Wang, *J. Phys. Chem. A*, 1999, **103**, 5889–5899.
- 11 B. Sirjean, P. A. Glaude, M. F. Ruiz-Lopez and R. Fournet, *J. Phys. Chem. A*, 2008, **112**, 11598–11610.
- 12 J. A. Miller, J. P. Senosiain, S. J. Klippenstein and Y. Georgievskii, *J. Phys. Chem. A*, 2008, **112**, 9429–9438.
- 13 J. M. Hostettler, L. Castiglioni, A. Bach and P. Chen, *Phys. Chem. Chem. Phys.*, 2009, **11**, 8262–8265.
- 14 Y. L. Yung, M. Allen and J. P. Pinto, *Astrophys. J., Suppl. Ser.*, 1984, **55**, 465–506.
- 15 Z.-X. Wang and M.-B. Huang, *Chem. Phys. Lett.*, 1998, **291**, 381–386.
- 16 R. K. Gosavi, I. Safarik and O. P. Strausz, *Can. J. Chem.*, 1985, **63**, 1689–1693.
- 17 M. R. Berman, J. W. Fleming, A. B. Harvey and M. C. Lin, *Chem. Phys.*, 1982, **73**, 27–33.
- 18 A. Canosa, I. R. Sims, D. Travers, I. W. M. Smith and B. R. Rowe, *Astron. Astrophys.*, 1997, **323**, 644–651.
- 19 H. Thiesemann, E. P. Clifford, C. A. Taatjes and S. J. Klippenstein, *J. Phys. Chem. A*, 2001, **105**, 5393–5401.
- 20 K. McKee, M. A. Blitz, K. J. Hughes, M. J. Pilling, H.-B. Qian, A. Taylor and P. W. Seakins, *J. Phys. Chem. A*, 2003, **107**, 5710–5716.
- 21 J.-C. Loison and A. Bergeat, *Phys. Chem. Chem. Phys.*, 2009, **11**, 655–664.
- 22 F. Goulay, A. J. Trevitt, G. Meloni, T. M. Selby, D. L. Osborn, C. A. Taatjes, L. Vereecken and S. R. Leone, *J. Am. Chem. Soc.*, 2009, **131**, 993–1005.
- 23 C. Chen, B. Braams, D. Y. Lee, J. M. Bowman, P. L. Houston and D. Stranges, *J. Phys. Chem. A*, 2011, **115**, 6797–6804.
- 24 C. Chen, B. Braams, D. Y. Lee, J. M. Bowman, P. L. Houston and D. Stranges, *J. Phys. Chem. Lett.*, 2010, **1**, 1875–1880.
- 25 P. Maksyutenko, F. Zhang, X. Gu and I. Kaiser Ralf, *Phys. Chem. Chem. Phys.*, 2011, **13**, 240–252.
- 26 X. Gu, Y. Guo, E. Kawamura and R. I. Kaiser, *J. Vac. Sci. Technol., A*, 2006, **24**, 505–511.
- 27 X. Gu, Y. Guo, F. Zhang, A. M. Mebel and R. I. Kaiser, *Faraday Discuss.*, 2006, **133**, 245–275; discussion 347–274, 449–252.
- 28 Y. Guo, X. Gu, E. Kawamura and R. I. Kaiser, *Rev. Sci. Instrum.*, 2006, **77**, 034701.
- 29 F. Zhang, S. Kim and R. I. Kaiser, *Phys. Chem. Chem. Phys.*, 2009, **11**, 4707–4714.
- 30 R. I. Kaiser, P. Maksyutenko, C. Ennis, F. Zhang, X. Gu, S. P. Krishtal, A. M. Mebel, O. Kostko and M. Ahmed, *Faraday Discuss.*, 2010, **147**, 429–478.
- 31 M. Vernon, *PhD thesis*, University of California, Berkeley, 1981.
- 32 M. S. Weiss, *PhD thesis*, University of California, Berkeley, 1986.
- 33 R. I. Kaiser, Y. T. Lee and A. G. Suits, *J. Chem. Phys.*, 1996, **105**, 8705–8720.
- 34 R. D. Levine, *Molecular Reaction Dynamics*, Cambridge University Press, Cambridge, UK, 2005.
- 35 W. B. Miller, S. A. Safron and D. R. Herschbach, *Discuss. Faraday Soc.*, 1967, **44**, 108–122.
- 36 F. Zhang, Y. Guo, X. Gu and R. I. Kaiser, *Chem. Phys. Lett.*, 2007, **440**, 56–63.